



Performance of multiple micro-perforated panels in a duct

Y. LIU¹; Y.S. CHOY²; Y.K. CHIANG³

^{1,2,3} Department of Mechanical Engineering, The Hong Kong Polytechnic University, HKSAR

ABSTRACT

Generalized formulation is developed analytically to calculate the transmission loss performance of a silencer by using multiple micro-perforate panel (MPP) array silencers in ventilation duct system. The device, based on single MPP design, consists of different expansion chambers with the side-branch cavities covered by micro-perforate panels of different properties. The theoretical model can also be simplified to evaluate the performance for normal plate silencer. With a preliminary result of two normal plates, it shows that the plate silencer can offer a wide stop band of 3.5 from low to medium frequency range when the length ratio is 1 to 4. Compared with same total length of a single plate, the stop band is improved by 25%. For the MPP silencer under similar condition, the stop band is also increased by 16%. Apart from the considerable increment of stop band, the bending stiffness requirement is also released by 35% and 40% respectively.

Keywords: Sound reflection, multiple panel, transmission loss
I-INCE Classification of Subjects Number(s): 26.1

1. INTRODUCTION

Designing a compact silencer which copes with broadband noise reduction, from very low to high frequency is still a technical challenging. The traditional dissipative method, such as the duct lining with fibrous material or porous absorber (1, 2) can give a desirable performance at mid to high frequencies but is ineffective at low frequencies due to its high magnitude of impedance. Although active noise control has the potential advantage of controlling low-frequency noise, issues related to reliability and cost remains a problem on wide-spreading its application in industry. Ultimately, the passive noise control approach is still more attractive from the view of application. Regarding the passive noise control method, there has been several noticeable developments. Based on the basic concept of resonator and expansion chamber, a more sophisticated technology of using the expansion chamber incorporating perforated panels has been explored would have a more broadband performance but they tend to be bulky and cause pressure losses. The pressure loss may cause extra energy consumption and more self-noise. Aiming at elimination of pressure loss, design of a compact, broadband noise control device, a silencer (3-5) which composed of two membranes or panels covered with two rectangular cavities has been developed and they are so called drum silencer or plate silencer respectively. Noise comes from the sound source in the duct of the ventilation system and excites the plates to vibrate with transverse displacement for the plate silencer. The vibration radiates sound which imposes a radiation pressure on the plate surface. There is a high coupling between the acoustic field in the duct and plate vibration. The sound radiates from the panels to the upstream due to the vibration is regarded as sound reflection wave. The increase of sound reflection implies the enhancement of transmission loss. The strong sound reflection capability relies on the domination of the first and the second modes of plate vibration. In order to achieve this, the most desirable structural properties of the plate inside the silencer are high bending stiffness but low density. It is difficult to obtain such kind of panel from traditional homogenous engineering materials. Therefore Choy et. al (6, 7) has developed a method of manufacturing a composite panel which composed of PMI foam with reinforcement of carbon fibre tows with very

¹ antonylau08@gmail.com

² mmyschoy@polyu.edu.hk

³ kidencyk@gmail.com

high strength- to-weight ratio. On the other hand, in order to widen the stopband and release the harsh requirement of the panel with high bending stiffness, recently a hybrid silencer has been proposed by introducing micro-perforations into a very light and moderately stiff plate. The purpose of the micro-perforations is to add sound absorptions to compensate for the deficiency in the passband caused by the insufficient sound reflection due to the plate with weaker strength to mass ratio. This hybrid silencer differs from the existing plate silencer in that sound reflection and absorption take dominant effect at different frequency ranges to provide a more uniformed TL curve.

Aiming for the achievement of high transmission loss and optimal bandwidth of the drum silencer, the membranes should be highly tensioned such that the first two in *vacuo* modes are dominant in the sound induced membrane vibration to improve the efficiency for sound reflection. However, it is practically difficult to implement that sufficiently high level of tension. Choy and Huang (8) have reduced the tension required for generating sufficient sound reflection in low frequency regime by the means of a partitioned silencer which divides the long membrane into two or more pieces. In other words, it breaks up a single drum silencer into multiple silencers. The required tension decreases drastically since the optimal tension of the partitioned membrane is proportional to the third power of the length. The similar concept is also applied to the micro-perforated panel absorbers in order to improve the performance of the traditional dissipative muffler with a broader applicable frequency range. Allam and Abom (9) proposed to insert rigid walls in the side-branched cavities of the MPP muffler such that the classical muffler is divided into a series of micro-perforated tubes in order to eliminate of minima in the transmission loss. The study provided good agreement between the simulated and measured results to verify that a broader bandwidth in transmission loss is accomplished by separating the single dissipative mufflers into multiple one. Due to the acoustic benefits obtained from the parallel arranged multiple MPP absorbers, Wang and Huang (10) further developed it with different cavity depths which is so-called MPP absorber array. The numerical results showed that the MPP absorber array enhances the absorption performance of micro-perforated panel with lower required optimal acoustic resistance. This acoustic absorption enhancement is caused by the strong resonance since the reactance matching conditions are different for each individual MPP absorber under unequal cavity depths. Moreover, the absorber array consists of different resonance frequency bands, and thus, a broader absorption bandwidth is achieved. The related previous study only investigated the performance of the multiple silencers and absorbers by assuming the separation between each chamber is small. Hence, the prediction of performance of the multiple silencers is achieved by neglecting the near field fluid loading created by adjacent silencer. However, in order to provide a more comprehensive understanding of the acoustic properties and performance of sound suppression of the multiple silencers, the effects of the gap between the silencer modules should also be studied as each silencer is possible to create cross interactions with the neighboring and causes a different response of the multiple silencers.

In what follows, Sec. 2 devotes to the description of the generalized 2D analytical model of the multiple panel configuration in detail. In Sec. 3, the optimal performance of the silencer is discussed for two panels with and without perforations. The effect of interval length between every two panels on the noise reduction is considered. In addition, the performance is also analyzed in terms of the response of the panels and sound radiation. Finally the main conclusions are summarized in Sec. 4.

2. PREDICTION FOR MULTIPLE MICRO-PERFORATE PANEL ARRAY

The proposed two-dimensional configuration of serial multiple micro-perforate panel (MPP) array is illustrated in Fig.1. This device consists of a serial of N fixed MPPs covering a side-branch rigid-walled cavity in an otherwise rigid-walled duct with a height h . The MPPs are separated by a simple segment of uniform duct with the interval length $g_{n,n+1}$ ($n=1,2,3\dots$) between every two panels, which is considered for installing the panel in practice. Each panel has a length of L_J ($J=1,2,3\dots$) and a bending stiffness of B_J ($J=1,2,3\dots$). For convenience, all parameters are normalized by a set of three basic quantities: air density ρ_0 , speed of sound c_0 , and the duct height h . So, the frequency f is normalized by c_0/h , bending stiffness per unit length B_J by $\rho_0 c_0^2 h^3$, plate mass per unit area m by $\rho_0 h$.

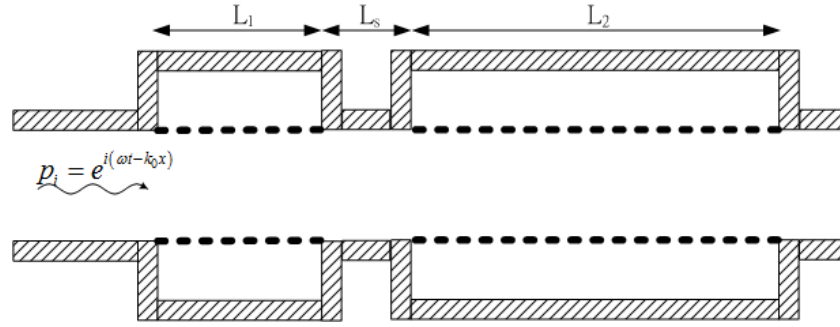


Figure 1 – Dual plate MPP silencer

Assuming the plate is in a harmonic motion, $v_{J,p} = \partial \eta_J / \partial t = i\omega \eta_J$, then dimensionless MPP vibration is governed by the following equation for the J th lower MPP,

$$\frac{B_J}{i\omega} \frac{\partial^4 v_{J,p}}{\partial x^4} + mi\omega v_{J,p} + P_{in} + P_{+rad} - P_{cavity,J} = 0 \quad (1)$$

where $P_{+rad} = \sum_{n=0}^{J-1} P_{+rad,Jn} + P_{+rad,J} + \sum_{J+1}^N P_{+rad,Jn}$. P_{in} is the incidence sound wave, P_{+rad} and $P_{cavity,J}$ are the fluid loading on the upper ($y=0+$) and lower sides ($y=0-$) of the MPP. Note that P_{+rad} is composed of three individual parts, which are sound radiation from both left and right sides of the J th plate, and radiation from the J th plate itself respectively.

In order to describe the air particle motion inside the MPP orifices, the averaged velocity field of the overall MPP surface is employed as below (11),

$$V_J = (1-\sigma)v_{J,p} + \sigma v_{J,0} = (1-\sigma)v_{J,p} + \overline{v_{J,0}} \quad (2)$$

where σ is the perforation ratio and $v_{J,0}$ is the spatially averaged velocity inside the hole of the J th panel. Since the hole diameter is much smaller than the acoustic wavelength of interest, the air particle velocity is assumed to be distributed uniformly within the area of each hole and the air-solid interface depends on a relative velocity relation $v_{J,p} - v_{J,0}$. Then the air-solid interaction related to the acoustic impedance is given by (11)

$$Z_{rs,0}(v_{J,0} - v_{J,p}) + Z_{ra,0}v_{J,0} + P_{in} + P_{+rad} - P_{cavity,J} = 0 \quad (3)$$

where $Z_{rs,0}$ and $Z_{ra,0}$ are the resistance and reactance of the MPP respectively, which are proposed by Maa (12) as

$$\begin{aligned} Z_0 &= Z_{rs,0} + Z_{ra,0} \\ &= \frac{32\mu\tau}{\rho_0 c_0 (d)^2} \left[\left(1 + \frac{K^2}{32}\right)^{0.5} + \frac{\sqrt{2}Kd}{32\tau} \right] + \frac{i\omega\tau}{c_0} \left[1 + \left(1 + \frac{K^2}{32}\right)^{-0.5} + 0.85 \frac{d}{\tau} \right] \end{aligned} \quad (4)$$

where τ is the thickness of the plate, d is the diameter of the hole, and μ is the coefficient of viscosity, $K = d\sqrt{\rho_0\omega} / \mu / 2$.

The dynamic response of the MPP expressed in Eqs.(1) and (3) can be solved by the standard Galerkin procedure. Note that in the following solution, the coordination system will be shifted on each plate as a simple trick by

$$\xi_J = \frac{x_J - \sum_{n=0}^{J-1} (L_n + g_{n,n+1})}{L_J}, \quad J=1,2,3,\dots \quad (5)$$

$v_{J,p}$ is therefore expanded as a series of *in-vacuo* mode $\phi_p(\xi)$ of the clamped-clamped plates with modal amplitude $V_{J,p}$

$$v_{J,p} = \sum_{p=1}^{\infty} V_{J,p} \phi_p(\xi_J), \quad V_{J,p} = \frac{1}{L_J} \int_0^1 v_{J,p} \phi_p d\xi_J \quad (6)$$

where

$$\phi_p(\xi) = (1 - \varepsilon_p) e^{\lambda_p \xi} / 2 + (1 + \varepsilon_p) e^{-\lambda_p \xi} / 2 + \varepsilon_p \sin(\lambda_p \xi) - \cos(\lambda_p \xi),$$

with

$$\varepsilon_p = \frac{\cosh(\lambda_p) - \cos(\lambda_p)}{\sinh(\lambda_p) - \sin(\lambda_p)}, \quad \cos(\lambda_p) \bullet \cosh(\lambda_p) = 1.$$

Owing to the orthogonal property of $\phi_p(\xi)$, Eqs. (1) and (3) then turn into

$$\left\{ \frac{B_J}{i\omega} \left(\frac{\lambda_p}{L_J} \right)^4 + mi\omega \right\} V_{J,p} + \int_0^1 (P_{in} + P_{+rad} - P_{cavity,J}) \phi_p(\xi_J) d\xi_J = 0 \quad (7)$$

and

$$Z_{rs,0} (V_{J,0,p} - V_{J,p}) + Z_{ra,0} V_{J,0,p} + \int_0^1 (P_{in} + P_{+rad} - P_{cavity,J}) \phi_p(\xi_J) d\xi_J = 0. \quad (8)$$

The integrations of the fluid loading component are employed as below,

$$\int_0^1 (P_{in} + P_{+rad} - P_{cavity}) \phi_p(\xi) d\xi = I_{J,p} + Z_{J,rad} - Z_{J,cav} \quad (9)$$

where $Z_{J,rad}$ and $Z_{J,cav}$ denotes the modal impedance contributed to the J th panel by the sound radiation inside the duct and cavity respectively, and $I_{J,p}$ denotes the modal coefficient of the incident wave on the J th panel, defined as

$$I_{J,p} = \int_0^1 p_i \phi_j(\xi_j) d\xi_j \quad (10)$$

For a duct of infinite length, the radiated sound caused by the vibration of the plate in the duct is (13):

$$P_{J,+rad}(x, y) = \frac{L_J}{2} \sum_{n=0}^{\infty} c_n \psi_n(0) \int_0^1 \psi_n(0) V(x_j') \times [H(x - x_j') e^{-ik_n(x-x_j')} + H(x_j' - x) e^{+ik_n(x-x_j')}] d\xi_j' \quad (11)$$

where $c_n = i / \sqrt{(n\pi / \omega)^2 - 1}$, $\psi_n(y) = \sqrt{2 - \delta_{0n}} \cos(n\pi y / h)$,

H is the Heaviside function and δ_{ij} is the Kronecker delta function.

Considering the MPP array configuration in the present study, the sound radiation pressure on the J th panel inside the duct is further divided into three parts, namely radiation from both left and right sides, and from the J th panel itself. Therefore, the modal impedance of sound radiation inside the duct can be rewritten as,

$$Z_{Jlt,rad,pq} = L_J \int_0^1 \sum_{n=0}^{\infty} c_n \psi_n(0) \int_0^1 \psi_n(0) V(x_j') \times [e^{-ik_n(x-x_j')}] d\xi_j' \phi_q(\xi_J) d\xi_J \quad (12)$$

for the sound radiation from left side of the J th panel,

$$Z_{Jrt,rad,pq} = L_J \int_0^1 \sum_{n=0}^{\infty} c_n \psi_n(0) \int_0^1 \psi_n(0) V(x_j') \times [e^{+ik_n(x-x_j')}] d\xi_j' \phi_q(\xi_J) d\xi_J \quad (13)$$

for the sound radiation from right side of the J th panel,

$$Z_{J,rad,pq} = L_J \int_0^1 \sum_{n=0}^{\infty} c_n \psi_n(y) \int_0^1 \psi_n(y) V(x') \times [H(x - x') e^{-ik_n(x-x')} + H(x' - x) e^{+ik_n(x-x')}] d\xi' \phi_q(\xi_J) d\xi_J \quad (14)$$

for the sound radiation from the J th panel itself.

The sound pressure inside the cavity $P_{J,cav}$ can be expressed in terms of the acoustic modes of a rigid-walled cavity with a light damping as

$$P_{J,cav} = \sum_{m,n} \frac{-i\omega \phi_{m,n}(x, y)}{L_J h_c (\kappa_{m,n}^2 - k^2 + 2i\zeta_{m,n} \kappa_{m,n} k)} \int_0^1 V(x', 0) \phi_{m,n}(x', 0) d\xi_j' \quad (15)$$

where L_J is the J th cavity length and h_c is the cavity depth, ζ_{mn} is the damping ratio of the (m, n) th acoustic mode $\psi_{mn}(x, y)$, and κ_{mn} the corresponding acoustic wave number of the acoustic mode $\psi_{mn}(x, y)$, with $\psi_{mn}(x, y)$ and κ_{mn} given as

$$\psi_{m,n}(x, y) = \sqrt{(2 - \delta_{0m})(2 - \delta_{0n})} \cos\left(\frac{m\pi x}{L_J}\right) \cos\left(\frac{n\pi y}{h_c}\right), \quad \kappa_{m,n}^2 = \left(\frac{m\pi}{L_J}\right)^2 + \left(\frac{n\pi}{h_c}\right)^2$$

Then the modal impedance from the sound radiation inside the J th cavity is obtained as

$$Z_{J,cav} = \int_0^1 p_{cav}(x, y) \phi_q(\xi_j) d\xi_j.$$

Finally, for simple presentation, let

$$Z_{J,rad-cav} = Z_{J,rad} - Z_{J,cav} \quad \text{and} \quad L_{J,pp} = \frac{B_J}{i\omega} \left(\frac{\lambda_p}{L_J} \right)^4 + mi\omega \quad (16)$$

The solution of Eqs. (7) and (8) can be cast into the following matrix in terms of modal vibration as:

$$\begin{bmatrix} L_{1,pp} + Z_{1,rad-cav}(1-\sigma) & \sigma Z_{1,rad-cav} & Z_{2,rad}(1-\sigma) & \sigma Z_{2,rad} & Z_{3,rad}(1-\sigma) & \sigma Z_{3,rad} \cdots \\ -Z_{rs,0} + Z_{1,rad-cav}(1-\sigma) & Z_{rs,0} + Z_{ra,0} + \sigma Z_{1,rad-cav} & Z_{2,rad}(1-\sigma) & \sigma Z_{2,rad} & Z_{3,rad}(1-\sigma) & \sigma Z_{3,rad} \cdots \\ Z_{1,rad}(1-\sigma) & \sigma Z_{1,rad} & L_{2,pp} + Z_{2,rad-cav}(1-\sigma) & \sigma Z_{2,rad-cav} & Z_{3,rad}(1-\sigma) & \sigma Z_{3,rad} \cdots \\ Z_{1,rad}(1-\sigma) & \sigma Z_{1,rad} & -Z_{rs,0} + Z_{2,rad-cav}(1-\sigma) & Z_{rs,0} + Z_{ra,0} + \sigma Z_{2,rad-cav} & Z_{3,rad}(1-\sigma) & \sigma Z_{3,rad} \cdots \\ Z_{1,rad}(1-\sigma) & \sigma Z_{1,rad} & Z_{2,rad}(1-\sigma) & \sigma Z_{2,rad} & L_{3,pp} + Z_{3,rad-cav}(1-\sigma) & \sigma Z_{3,rad-cav} \cdots \\ Z_{1,rad}(1-\sigma) & \sigma Z_{1,rad} & Z_{2,rad}(1-\sigma) & \sigma Z_{2,rad} & -Z_{rs,0} + (Z_{3,rad-cav})(1-\sigma) & Z_{rs,0} + Z_{ra,0} + \sigma Z_{3,rad-cav} \cdots \end{bmatrix} \begin{bmatrix} V_{1p} \\ V_{1,0,p} \\ V_{2p} \\ V_{2,0,p} \\ V_{3p} \\ V_{3,0,p} \\ \vdots \end{bmatrix} = - \begin{bmatrix} I_{1p} \\ I_{1p} \\ I_{2p} \\ I_{2p} \\ I_{3p} \\ I_{3p} \\ \vdots \end{bmatrix} \quad (17)$$

As a result, $V_{J,p}$ and $V_{J,0,p}$ can be solved through matrix inversion. In addition, the transmission loss (TL) to the duct downstream can be calculated by taking the sound radiation of only the plane wave mode $n=0$ from all the MPPs as:

$$TL = -20 \log_{10} \left(1 + \frac{\sum_{j=1}^N P_{+rad,j}(x,y) \Big|_{n=0, x \rightarrow +\infty}}{P_i} \right).$$

3. ANALYSIS OF THE MULTIPLE PANEL PERFORMANCE

3.1 Performance of dual-plate without perforations

The optimal TL spectrum of a two-plate configuration is shown first in Fig.2(a). It can be seen from the top figure of Fig.2(a) that compared with single plate silencer, by using two-plate configuration the optimized maximum frequency band increases by about 15% from 2.81 to 3.22. Although the lower limit increases from 0.0445 to 0.061, the upper frequency limit increases significantly from 0.125 to 0.197. Such frequency increment in bandwidth probably comes from the reduction of the maximum individual plate length in a two-plate configuration. Fig.2 (b)-(d) display the stopband contour as a function of bending stiffness for different plate length combinations. It can be observed that as far as the plate length combination considered here, the maximum stopband ranges from 2.6 to 3.2. Thus the optimal plate lengths are 1 and 4, and the corresponding bending stiffness are 0.002 and 0.038, respectively. Compared to the single clamped plate silencer, the bending stiffness requirement can drop from 0.069 to 0.038 by about 45%, which is very attractive.

In order to further understand the noise reduction performance, the plate response and the first fourth modal reflection effect is analyzed in Fig.3. The IL spectrum is attached on the top of each column to facilitate the study of the peak and trough frequencies. The vibration response of each individual mode, $|V_{J,p}|$, is shown in the subfigures on the first and second row for the first and second plate respectively. It is obvious that the 1st vibration mode of the first plate ($L_1=1$) is very dominant in the middle frequency range from $f=0.13$ to 0.22. On the other hand, the 1st and 2nd vibration modes of the second plate ($L_2=4$) are more prominent in the low frequency range below $f=0.14$. As far as the frequency range of interest is concerned, all the three kinds of vibration mode are strong at high frequency range above $f=0.22$. Therefore, the good performance of the noise reduction for the two-plate configuration benefits from the strong responses of the 1st modal vibration of the first plate and the first two modal vibrations of the second plate. The combination of the different responses sustains the high TL performance through the whole frequency range of interest.

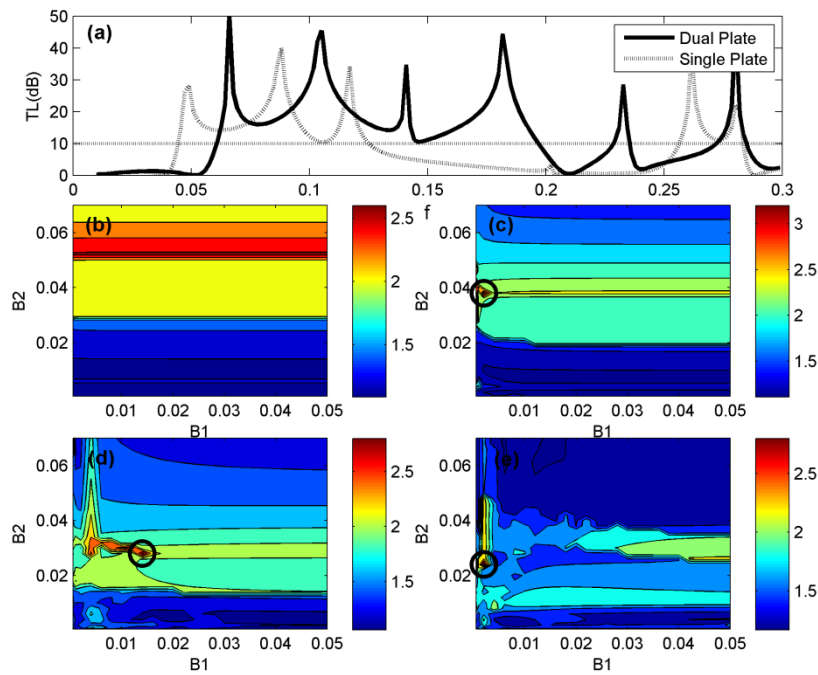


Figure 2 - Optimized plate length and the optimal spectrum. The top figure is the TL spectrum at the optimal bending stiffness. The subfigures show the optimal stopband contour as a function of different bending stiffness for different plate length combination (a) $L_1=0.5, L_2=4.5$ (b) $L_1=1, L_2=4$ (c) $L_1=1.5, L_2=3.5$ (d) $L_1=2, L_2=3$.

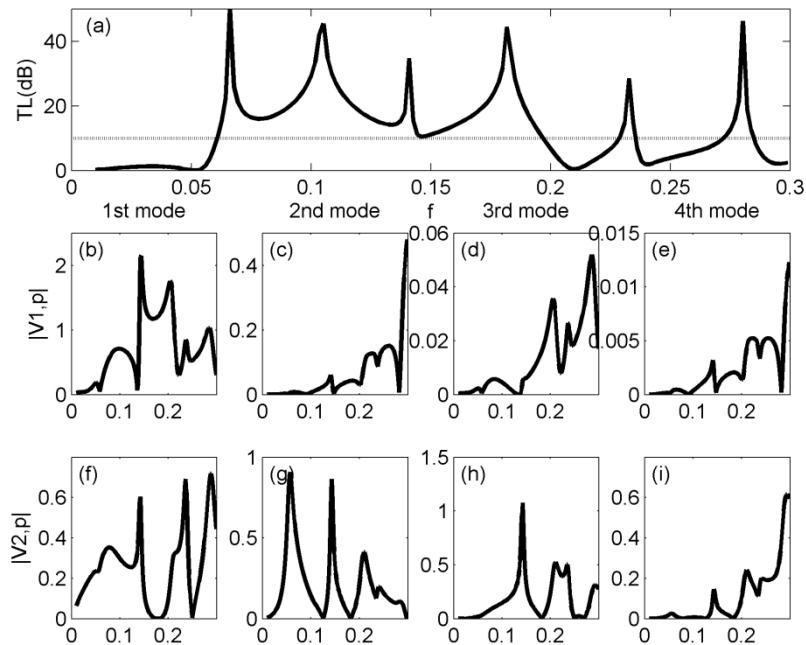


Figure 3 - Modal radiations. The top figure is the TL spectrum at the optimal bending stiffness. The subfigures in the first row are the modal vibration amplitude $|V_j|$ for the first plate, the modal vibration amplitude $|V_j|$ in the second row are for the second plate.

3.2 Interval length effect on the performance of dual-plate silencer

The interval length between every two plates is necessary for installing the plates of such a plate array configuration in practice. In the present theory, this length will affect the pressure loading on one panel from another as shown in Eqs. (13) and (14). In order to explore the length effect on the performance, the selection of the interval length is considered in this part. Fig.4 (a) illustrates the spectrum variation when the interval length increases under the optimized plate properties. In the frequency bandwidth of interest, the existence of trough point near $f=0.15$ leads to the stopband to be only 2.35. However, as the length increases, this trough point can disappear at $L_s=0.5$ and 4, and be shifted to another frequencies at $L_s=2$ and 10. Such variation of trough point directly causes a stopband change as displayed Fig. 4(b). It is seen that basically the stopband experiences a repeated pattern, and when $L_s=4$ the stopband reaches as high as 3.64 which is a 30% increment compared with the single plate silencer. Besides, the stopband can sustain high within a small variation range of 0.4 near this length. Similar phenomena is observed at the second high stopband when $L_s=0.5$. Such variation of interval length can accommodate some unavoidable changes in practice, for example the manufacturing accuracy, and demonstrates the robustness of the silencer.

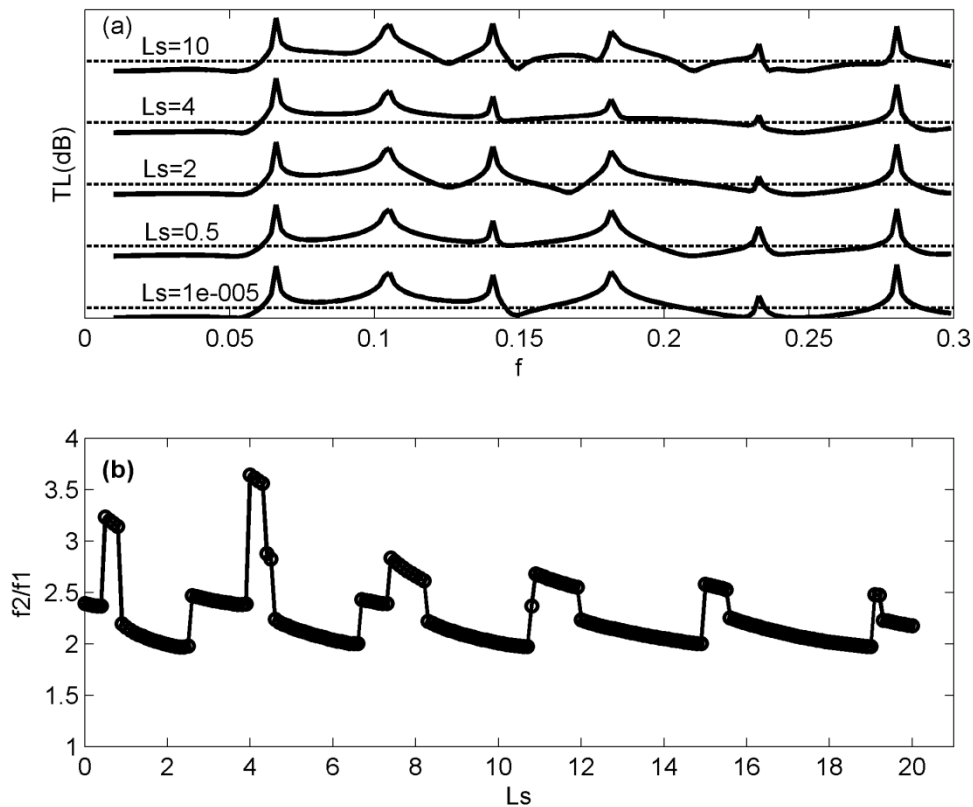


Figure 4 - (a) Transmission loss spectrum as function of interval length (Fixed $L_1=1, L_2=4, B_1=0.002, B_2=0.038$), (b) Stopband variation with interval length.

To understand the mechanism of the performance change due to the interval length effect, the modal impedance of the cross interactions between different plates defined in Eq. (12) and (13) are analyzed in Fig. 5. Several observations are discussed here based on the first two modal impedance spectrum. First, the modal impedance of cross interactions from one plate to another possesses more periods when L_s increases; second, the modal impedances share the same pattern for each mode but have different amplitudes; last but not the least, the modal impedance becomes to be vanish around $f=0.15$ when $L_s=0.5$ and 4. The zero impedance indicates the strong sound reflections from the first two dominant vibrations at this frequency point hence a TL improvement. Related to the stopband variation, this cross modal impedance plays an important role in determining the TL at around $f=0.15$ and stopband performance.

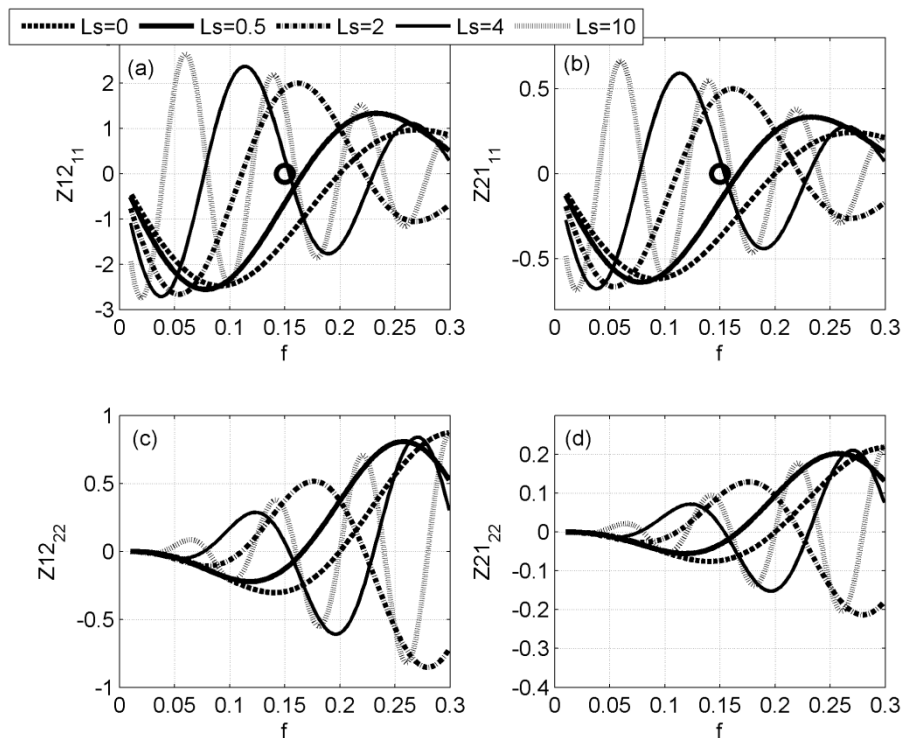


Figure 5 - Reactance of the first and second modes from one plate to another. (a) and (c) Show the component variation of the first and second mode reactance against frequency from the second plate to the first plate with different interval lengths. (b) and (d) Show the similar curves from the first plate to the second plate.

3.3 Performance of dual-MPP configuration

Similar optimization procedure is employed for a two-MPP configuration in the second step. Note that the following parameters of MPP properties (14) are used in the calculation: $\tau=0.04$, $d=0.005$, and $\sigma=0.5\%$. Fig. 6(a) compares the TL spectrum of a two-MPP configuration under the optimal condition with that of a two-plate one with the same plate length and bending stiffness. The optimized MPP length is 1 to 4 with bending stiffness of 0.004 and 0.034 respectively. It is clear that the frequency bandwidth of the two-MPP configuration can be as broad as 4.14 with the lower and upper limits are 0.058 and 0.24 respectively. For the performance of a single MPP silencer (14), the lower and upper frequency limits and stopband are 0.044, 0.124 and 2.81 respectively. Obviously, the optimal performance of the two-MPP configuration is much better than that of the single MPP silencer with an increment of 47% in terms of the achievable stopband. Compared with the two-plate silencer with same plate length and bending stiffness, the TL is improved near $f=0.13$ and frequency above $f=0.15$ when using two-MPP configuration. The two rows of subfigures below the spectrum compare the vibration response of each individual mode $|V_{j,p}|$. In general, the dominant modal reflections of both plate and MPP silencer share nearly the same contributions from the 1st modal vibration of the first panel and first two modal response of the second panel. It can also be seen that the high TL in the frequency range of $f=0.13$ to 0.23 are mainly due to the high response of the 3rd and 4th modal vibration as shown in Figs.6(d) and (e), however, such modal vibrations are very weak on the two-plate silencer. Apart from these two modes, the vibration peaks are reduced and smoothed compared with the pure plate silencer. Previous study reveals that the vibration reduction mainly results from the introduction of the micro-perforations that brings about a certain degree of pressure balance across the perforated panel through the holes.

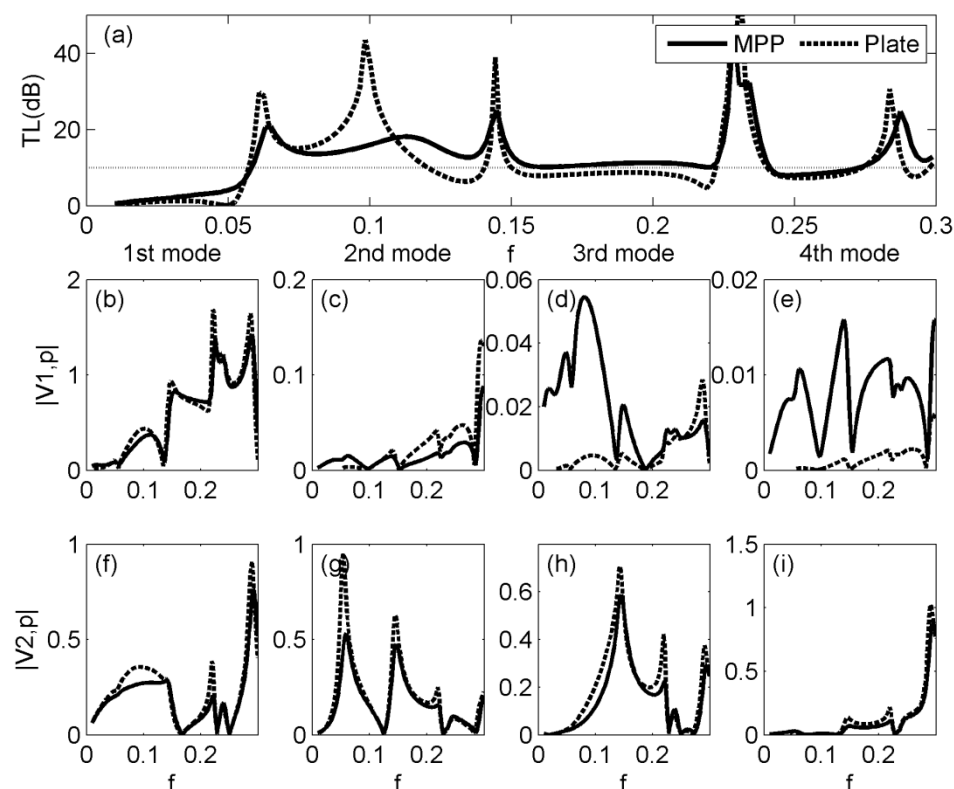


Figure 6 - Spectrum and modal radiations. The top figure is the TL spectrum at the optimal bending stiffness for the two-panel configuration with/without perforations. The subfigures in the first row are the modal vibration amplitude $|V_j|$, the subfigures in the second row are the modal vibration amplitude $|V_j|$ for the second plate.

4. CONCLUSIONS

The sound transmissions across a duct section with the wall-mounted arrays consisting of multiple plate silencers with or without micro-perforations are investigated analytically. Analyses have been conducted to understand the vibro-acoustics mechanisms and cross coupling effect between the plates. The findings of the current study are summarized as follows:

1. A theoretical model of the array of plate silencers with or without perforations has been developed. It involves the coupling between the plates with different mass and bending stiffness.
2. For the dual plate silencer, the optimal plate lengths ratio is 1:4 and the corresponding bending stiffness are 0.002 and 0.038, respectively. Compared to the single clamped plate silencer, the bending stiffness requirement can drop from 0.069 to 0.038 by about 45%. At the same time, the stopband can be enhanced by about 30%.
3. The separation between the plate silencers crucially influences the cross coupling between

the adjacent plates and thus the sound radiation will also be affected.

ACKNOWLEDGEMENTS

The authors thank the General Research Grant for the funding support (BQ39B)

REFERENCES

1. Beranek LLVIL. Noise and vibration control engineering : principles and applications. New York: Wiley; 1992.
2. Ingard KU. Notes on sound absorption technology. Poughkeepsie, NY: Noise Control Foundation; 1994.
3. Huang L. Modal analysis of a drumlike silencer. *The Journal of the Acoustical Society of America*. 2002;112(5):2014-25.
4. Choy YS, Huang L. Experimental studies of a drumlike silencer. *The Journal of the Acoustical Society of America*. 2002;112(5):2026-35.
5. Huang L. Broadband sound reflection by plates covering side-branch cavities in a duct. *The Journal of the Acoustical Society of America*. 2006;119(5):2628-38.
6. Choy YS, Lau KT, Wang C, Chau CW, Liu Y, Hui D. Composite panels for reducing noise in air conditioning and ventilation systems. *Composites Part B: Engineering*. 2009;40(4):259-66.
7. Choy YS, Liu Y, Lau KT. Duct Noise Control by Using Very Light Composite Plate. *AMR Advanced Materials Research*. 2012;410:361-5.
8. Choy YS, Huang L. Multiple drumlike silencer for low frequency duct noise reflection. *Applied Acoustics*. 2009;70(11-12):1422-30.
9. Allam S, Å bom M. A New Type of Muffler Based on Microperforated Tubes. *Journal of Vibration and Acoustics*. 2011;133(3):031005-.
10. Wang C, Huang L. On the acoustic properties of parallel arrangement of multiple micro-perforated panel absorbers with different cavity depths. *The Journal of the Acoustical Society of America*. 2011;130(1):208-18.
11. Takahashi D, Tanaka M. Flexural vibration of perforated plates and porous elastic materials under acoustic loading. *The Journal of the Acoustical Society of America*. 2002;112(4):1456-64.
12. Maa DY. THEORY AND DESIGN OF MICROPERFORATED PANEL SOUND-ABSORBING CONSTRUCTIONS. *SCIENCE CHINA Mathematics*. 1975;18(1):55-71.
13. Doak PE. Excitation, transmission and radiation of sound from source distributions in hard-walled ducts of finite length (I): The effects of duct cross-section geometry and source distribution space-time pattern. *Journal of Sound and Vibration*. 1973;31(1):1-72.
14. Wang XN, Choy YS, Cheng L. Hybrid noise control in a duct using a light micro-perforated plate. *The Journal of the Acoustical Society of America*. 2012;132(6):3778-87.